

Magnetocapacitance effect in perovskite -superlattice based multiferroics

M.P. Singh, W. Prellier*, Ch. Simon and B. Raveau
*Laboratoire CRISMAT, CNRS UMR 6508, ENSICAEN,
6 Bd du Maréchal Juin, F-14050 Caen Cedex, FRANCE.*

(July 20, 2018)

Abstract

We report the structural and magnetoelectrical properties of $\text{La}_{0.7}\text{Ca}_{0.3}\text{MnO}_3/\text{BaTiO}_3$ perovskite superlattices grown on (001)-oriented SrTiO_3 by the pulsed laser deposition technique. Magnetic hysteresis loops together with temperature dependent magnetic properties exhibit well-defined coercivity and magnetic transition temperature (T_C) ~ 140 K. *DC* electrical studies of films show that the magnetoresistance (MR) is dependent on the BaTiO_3 thickness and negative *MR* as high as 30% at 100K are observed. The *AC* electrical studies reveal that the impedance and capacitance in these films vary with the applied magnetic field due to the magnetoelectrical coupling in these structures - a key feature of multiferroics. A negative magnetocapacitance value in the film as high as 3% per tesla at 1kHz and 100K is demonstrated, opening the route for designing novel functional materials.

*prellier@ensicaen.fr

Superlattices, which are composed of thin layers of two or more different structural counterparts that stacked in a well-defined sequence, may exhibit some remarkable properties that do not exist in either of their parent forms. For example, a $(\text{LaFeO}_3)/(\text{LaCrO}_3)$ superlattice stacked on (111)- SrTiO_3 exhibits a ferromagnetic behavior, whereas each parent material is antiferromagnetic¹. Similarly, many perovskite superlattices can exhibit new properties such as high temperature superconductivity². To grow these superlattices, various thin films techniques such as molecular beam epitaxy, chemical vapor deposition, pulsed laser deposition (PLD) technique *etc.* have been employed. In particular, the PLD process is one of the most suitable and frequently used techniques to grow the superlattice of multi-component perovskite oxides in a moderate oxygen pressure³.

A multiferroic is a material in which ferromagnetism and ferroelectricity coexist⁴. As a consequence, the magnetic domains can be tuned by the application of an external electric field, and likewise electric domains are switched by magnetic field. Thus, these materials offer an additional degree of freedom in designing the various devices, e.g. transducers, actuators, storage devices, which is unachievable separately in either ferroelectric or magnetic materials. Hitherto, a very few materials, e.g. perovskite-type BiFeO_3 , hexagonal REMnO_3 (RE=rare earths), and the rare-earth molybdates, exist in nature or synthesized in laboratory which exhibit multiferroism⁵⁻¹⁰. Note that most of these compounds display an antiferromagnetic behavior⁵⁻¹⁰. These non-trivial spin-lattice coupling in the multiferroics has been manifested through various forms, such as linear and bilinear magnetoelectric effects, polarization change through field-induced phase transition, magneto-dielectric effect, and dielectric anomalies at magnetic transition temperatures⁵⁻¹⁰. Why and under what circumstances a large coupling should come about is a major open question, but this problem has proved difficult to tackle owing to the lack of materials that show such large coupling. Also the absence of multiferroics with large coupling at moderate conditions is one of the big hurdles in the realization of multiferroic devices. Thus, it is essential to design novel multiferroic materials with essential properties. To synthesize these novel multiferroics, various efforts have been made by mixing the ferroelectric and magnetic materials in forms of

either composites or multilayers^{11,12} in view of possible applications.

In the present work, we have utilized the versatility of the PLD technique to create a multilayer structure in a superlattice form composed of a piezoelectric and ferroelectric, namely BaTiO₃ (BTO); and a ferromagnet, namely La_{0.7}Ca_{0.3}MnO₃ (LCMO). The superlattices were characterized by the various techniques for their structural, magnetic, electrical, and magneto-electrical properties, and our results are reported in this article.

Superlattices of BTO/LCMO were grown on (001)-oriented SrTiO₃ (STO) by the pulsed laser deposition technique, using stoichiometric targets, at 720°C in a flowing 100 mTorr oxygen atmosphere. Superlattices with individual BTO layer thickness of 1 to 25 unit cells (u.c.) by keeping the LCMO layer thickness as 5 u.c. were realized. The choice of 5 u.c. came because thin layer of LCMO behaves as a ferromagnetic insulator¹³. The superlattice is composed of 25 repeated units of BTO/LCMO bilayers with LCMO as the bottom layer.

The samples were characterized by X-ray diffraction (XRD) using Seifert 3000P diffractometer (Cu K α , $\lambda = 0.15406$ nm) and a Philips X'Pert for the in-plane measurements. Magnetization (M) was measured as a function of temperature (T) and magnetic field (H) using a superconducting quantum interference device magnetometer (SQUID). *DC* electrical resistivity (ρ) of films were measured in four probe configuration. *AC* electrical properties of the films were measured by a lock-in amplifier (Stanford Research 850) in the frequency range of 1-10⁶ Hz, where the sample was held in PPMS system. To measure the electrical properties of the films in current-perpendicular-to-the-plane (CPP) geometry, a LaNiO₃ electrode was fabricated through a shadow mask¹⁴.

In Fig. 1a, we show the $\Theta - 2\Theta$ XRD scan around the (002) fundamental peak (40°-52° in 2Θ) of 5 u.c. LCMO/ 10 u.c. BTO (denoted hereafter as 5/10) superlattice. The denoted number i indicates the i^{th} satellite peak. The presence of higher order satellite peaks adjacent to the main peak, arising from chemical modulation of multilayer structure, indicates that the films were indeed coherent heterostructurally grown. The periodic chemical modulation for the (5/10) superlattice, as extracted from $\Theta - 2\Theta$ XRD, is $\Lambda = 5.98$ nm which is in agreement with theoretical values (5.94 nm) based on the lattice parameters of each

constituent (0.386nm for LCMO and 0.4006nm for BTO). The full-width-at-half-maximum (FWHM) of the rocking curve, recorded around the fundamental (002) diffraction peak of the same superlattice, is very close to the instrumental broadening ($< 0.2^\circ$), indicating a well crystallinity and a good coherency (see inset of Fig1a). Further, to examine the in-plane coherence, Φ -scan was recorded around the 103 reflection of the cubic unit cell. Different Φ -scans (not shown here) were recorded by at various tilted angle leading to a pole figure. Four peaks are clearly observed at 90° from each other, indicating a four-fold symmetry as expected for the perovskite structures LCMO and BTO. This well defined pattern is an evidence for the in-plane texture of the superlattice. Similar scans recorded on other films confirm that the superlattices grow epitaxially on STO. The film morphology, examined by atomic force microscopy, gave a roughness in the range of 3-6Å (close to one perovskite u.c.) for all films showing that they have a very smooth surface.

Magnetization vs. applied magnetic field ($M - H$) loop and vs. temperature $M(T)$ measurements were performed on all samples and Fig.1b shows an example in-plane hysteresis loop for a (5/10) superlattice, recorded at 10K. The curve clearly shows a well-defined coercivity confirming the ferromagnetic nature of the film. Furthermore, the temperature-dependance of the magnetization $M(T)$ recorded under 3000Oe applied magnetic field, shows the magnetic transition from ferromagnetic to paramagnetic at T_C (Curie temperature) around 140K. This value is lower than the observed bulk LCMO (250K), but results from both the substrate-induced strain and the thickness of the layer (5 u.c.)^{15,16}. Surprisingly, the Curie temperature of the superlattices is almost independent of the BTO thickness layer (in the range 135-142K for all films). Despite the similarity in the shape of the hysteresis loop, the magnetic data reveal some differences. For example, the magnetization of the films is dependent on the thickness of BTO spacer layer (see inset of Fig.1b). A detailed study shows that the total magnetization of the films is increasing with increase in the BTO thickness up to 15 u.c. This is surprising because the LCMO thickness is constant throughout all the samples. Thus, it is possible to increase the magnetization only when the LCMO is inducing the magnetization in BTO layer via magnetoelectric coupling. With further

increase in BTO thickness (i.e. above 15 u.c.) magnetization is decreasing, which is mostly attributed to the variation in the strains, as previously reported for superlattices^{15,16}

Figure 2a displays the *DC* resistivity of (5/5), (5/10) and (5/15) superlattices which were measured as a function of temperature without magnetic field. The inset of Fig.2a displays the magnetic field-dependance of the magnetoresistance (*MR*) of a (5/15) superlattice taken at 100K. *MR* is defined as $MR (\%) = 100 \times [R(H) - R(0)]/R(0)$, where $R(H)$ and $R(0)$ are the resistance measured with and without magnetic field, respectively. Fig.2a clearly reveals that the resistivity is increasing with BTO thickness, which is consistent with the BTO insulating behavior. With increasing in the BTO layer thickness above 15 u.c., the resistance of the samples is indeed getting too large to measure above 100K, as it should be in BTO. This shows that the "magnetic" BTO is also more conducting than that of classical BTO.

In order to understand the coherent spin transport in these films, MR were measured for different samples. Fig. 3b shows the evolution of MR as a function of temperature for a (5/15) superlattice and inset of Fig. 3b shows the *MR* for several BTO thickness (from 5 to 25) measured at 100K. Fig.3b clearly indicates that with increasing temperature, the *MR* is increasing and vanishes above the transition temperature which is consistent with the LCMO property. Further, with increase in the BTO thickness up to 15 u.c. (Inset of Fig.3b), there is enhancement in *MR*. This is surprising because, the *MR* in a multilayer with an insulating barrier basically arises from the tunneling of coherent magnetic carriers and spin polarization of either side of the magnetic layer, i.e. magnetic layer thickness and structure, whereas in the present case the number of interfaces and magnetic layer thickness is constant for all superlattices.¹⁷. However, in principle the *MR* does not increase with increase of tunnel barrier thickness¹⁷. The enhancement in MR may be understood as follows. The total resistivity (ρ_{total}) of the samples can be expressed as $\rho_{total} = x \rho_{BTO} + (1 - x) \rho_{LCMO}$ where 'x' is the BTO compositional resistivity coefficient; ρ_{BTO} and ρ_{LCMO} is bulk resistivity of BTO and LCMO, respectively. Since the thickness of the LCMO as well as the number of interfaces are constant in all samples, the increase in the enhancement

MR will be arising from the BTO layer. Thus, it is evident that, up to 15 u.c., the BTO layer is magnetically polarized, which corroborates the ($M - H$) findings. Henceforth, the observed enhancement in magnetoresistance with the increase of BTO thickness may be attributed to the possible magnetoelectric coupling in these superlattices as previously seen for $(\text{Pr}_{0.85}\text{Ca}_{0.15}\text{MnO}_3)/(\text{Ba}_{0.4}\text{Sr}_{0.6}\text{TiO}_3)$ superlattices¹⁴. Furthermore, MR was diminishing with further increase in BTO thickness (i.e. above 15 u.c.), which is attributed to the loss of spin coherence due to the large tunnel barrier thickness. Thus, the above results (Fig.1b and Fig.2) clearly exhibit that the maximum magnetoelectric coupling can be expected in (5/15) superlattice.

In order to study the magnetoelectric coupling in these films, AC electrical properties were measured. Fig.3 shows the impedance (Z) vs frequency at different temperatures under 0T and 5T applied magnetic field, for a (5/15) superlattice. Two regimes are observed. Below 150K, the impedance of the sample decreases with applied magnetic field, whereas above 150K it vanishes and no significant variation is seen with magnetic field at higher temperatures (see Fig.3d). Further, we have extracted the capacitance of the film based on an equivalent parallel RC circuit, which has been chosen based on the Cole-Cole plot (not shown) of the observed impedance data. The estimated capacitance up to 150K is reported in the Fig 4. The capacitances vs. frequency curves exhibit the two important features. First, the capacitance of the sample is constant at low frequency and decreases with the progressive increase in frequency. In a given device dimension, the capacitance of the device dependence on the total electrical polarizability of the materials. There are the four electrical polarizability components, namely electronic, ionic, dipolar and space charge, and their contribution strongly depend on the frequencies¹⁸. At low frequency ($\sim 1\text{Hz} - 1\text{MHz}$), the contribution comes from all these components, whereas above 1kHz frequency it starts decreasing and the dipolar contribution becomes zero around 100MHz. Thus, the decrease of the capacitance at higher frequency indicates presence of electric dipoles in the film. Hence, it indirectly provides an evidence of the presence ferroelectricity in these films. Second, there is a decrease of the capacitance under applied magnetic fields. In the previous

reports, usually the magnetocapacitance effects have been shown near the Curie temperature. In the present case it occurs well below the Curie temperature and is significant large in magnitude. The magnetocapacitance MC is defined, by analogy to the MR as, $MC(T)$ (%) = $100 \times [C(H, T) - C(0, T)]/C(0, T)$, where $C(H, T)$ represents the capacitance at a magnetic field H and a temperature T . The negative MC value observed at 1kHz and 100K was $\sim 17\%$. The detail study reveals that the MC was less than 1% at 5K whereas it increases with increasing the temperature and diminishes above 150K. The MC effect, at low frequency (1kHz) is interesting since it shows that the superlattice can be considered as a new compound with novel properties that are not observed in both the parent compounds.

It clearly evidenced that the artificial structure is behaving as a multiferroic. Such effect was not reported on artificial superlattices. This effect is a *direct evidence of magnetoelectric coupling in the film*, as alluded above, and as reported in other multiferroics^{6-10,12}. However, it is worth to note that the magnetocapacitance effects in some ceramics of the hexagonal rare earth manganites are of the order of 1% *per tesla* near transition temperature (~ 40 K), whereas in the present case it is of the order of 3% *per tesla* at 100K. It should also be noticed that the MC effect appears only at low frequency. This can be understood if one uses the model already proposed in Ref.¹² where the BTO layer is replaced by a R and C in parallel, the LCMO as a single R . In this model, the MR of the BTO layer is in agreement with the MC at low frequency in the whole material.

To summarize, we have successfully grown high quality ($\text{BaTiO}_3/\text{La}_{0.7}\text{Ca}_{0.3}\text{MnO}_3$) superlattices on STO by PLD process. Despite the lattice mismatch between substrate and LCMO (-1.17%), and BTO (+2.2%), the films were grown heteroepitaxial. Magnetoelectrical measurements revealed that the films have at 100K, a negative magnetoresistance close to 4% *per tesla* and a negative magnetocapacitance effect of the order of 3% *per tesla* at 1kHz. The presence of the coupling between dielectric and magnetic orders have thusly been demonstrated. This high magnetocapacitance as well as the large magnetoresistance open a path in designing novel multiferroic thin films.

We would like to thank Prof. James N. Eckstein, Dr. L. Méchin, Prof. B. Mercey and

Ms. N. Bellido for helpful discussions.

This work has been carried out in the frame of the European Network of Excellence "Functionalized Advanced Materials Engineering of Hybrids and Ceramics" FAME (FP6-500159-1) supported by the European Community, and by Centre National de la Recherche Scientifique.

REFERENCES

- ¹ K. Ueda, H. Tabata, T. Kawai, *Science* **280**, 1064 (1998).
- ² D.P. Norton, B.C. Chakoumakos, J.D. Budai, D.H. Lowdes, B.C. Sales, J.R. Thompson, and D.K. Christen, *Science* **265**, 2704 (1994).
- ³ W. Prellier, B. Mercey, Ph. Lecoœur, J.F. Hamet, and B. Raveau, *Appl. Phys. Lett.* **71**, 782 (1997).
- ⁴ H. Schmid, *Ferroelectrics* **162**, 317 (1994).
- ⁵ A. Sharan, J. Lettieri, I. An, C. Chen, R.W. Collins, J. Lettieri, Y. Jia, D.G. Schlom, and V. Gopalan, *Appl. Phys. Lett.* **83**, 5169 (2004).
- ⁶ J. Wang, J.B. Neaton, H. Zheng, V. Nagarajan, S.B. Ogale, B. Liu, D. Viehland, V. Vaithyanathan, D.G. Schlom, U.V. Waghmare, N.A. Spaldin, K.M. Rabe, M. Wutting, and R. Ramesh, *Science* **299**, 1719 (2003).
- ⁷ B. Lorenz, F. Yen, M.M. Gospodivno, and C.W. Chu, *Phys. Rev. B* **71**, 014438 (2005).
- ⁸ P.A. Sharma, J.S. Ahn, N. Hur, S. Park, S.B. Kim, S. Lee, J.-G. Park, S. Guha, and S.-W. Cheong, *Phys. Rev. Lett.* **93**, 177202-1 (2004).
- ⁹ N. Hur, S. Park, P. A. Sharma, J. S. Ahn, S. Guha, and S-W. Cheong, *Nature* **429**, 392 (2004).
- ¹⁰ T. Kimura, S. Kawamoto, I. Yamada, M. Azuma, M. Takano, and Y. Tokura, *Phys. Rev. B* **67**, 180401(R) (2003); T. Kimura, T. Goto, K. Thizaka, T. Arima, and Y. Tokura, *Nature* **426**, 55 (2003).
- ¹¹ H. Zheng, J. Wang, S.E. Lofland, Z. Ma, L.M. Ardabili, T. Zhao, L.S. Riba, S.R. Shinde, S.B. Ogale, F. Bai, D. Viehland, Y. Jia, D.G. Schlom, M. Wutting, A. Roytburd, and R. Ramesh, *Science* **303**, 661 (2004).
- ¹² P. Murugavel, D. Saurel, W. Prellier, Ch. Simon, and B. Raveau, *Appl. Phys. Lett.* **85**,

- 4424 (2004).
- ¹³ M.G. Blamire, B.-S. Teo, J.H. Durrel, N.D. Mathur, Z.H. Barber, J.L.M. Driscoll, J.F. Cohen, and J.F. Evetts, *J. Magn. Magn. Mater.* **167**, 200 (1997).
- ¹⁴ P. Murugavel, P. Padhan, and W. Prellier *Appl. Phys. Lett.* **85**, 4992 (2004).
- ¹⁵ G.Q. Gong, A. Gupta, G. Xiao, P. Lecoeur, and T.R. McGuire, *Phys. Rev. B* **54**, R3742 (1996).
- ¹⁶ P. Padhan, W. Prellier, and B. Mercey, *Phys. Rev. B* **70**, 184419 (2004).
- ¹⁷ M.H. Jo, N.D. Mathur, J.E. Evetts, M.G. Blamire, M. Bibes, J. Fontcuberta, *Appl. Phys. Lett.* **75**, 3689 (1999).
- ¹⁸ A.R. West, *Solid State Chemistry and its Applications*, pp. 534-537 (John Willey and Sons, New York, 1984).

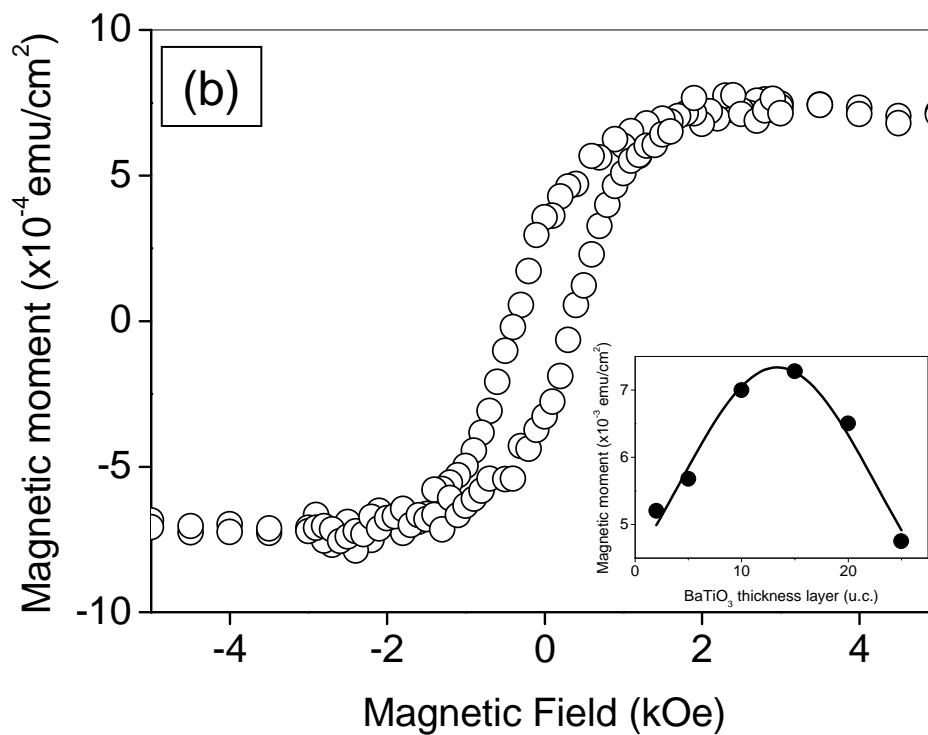
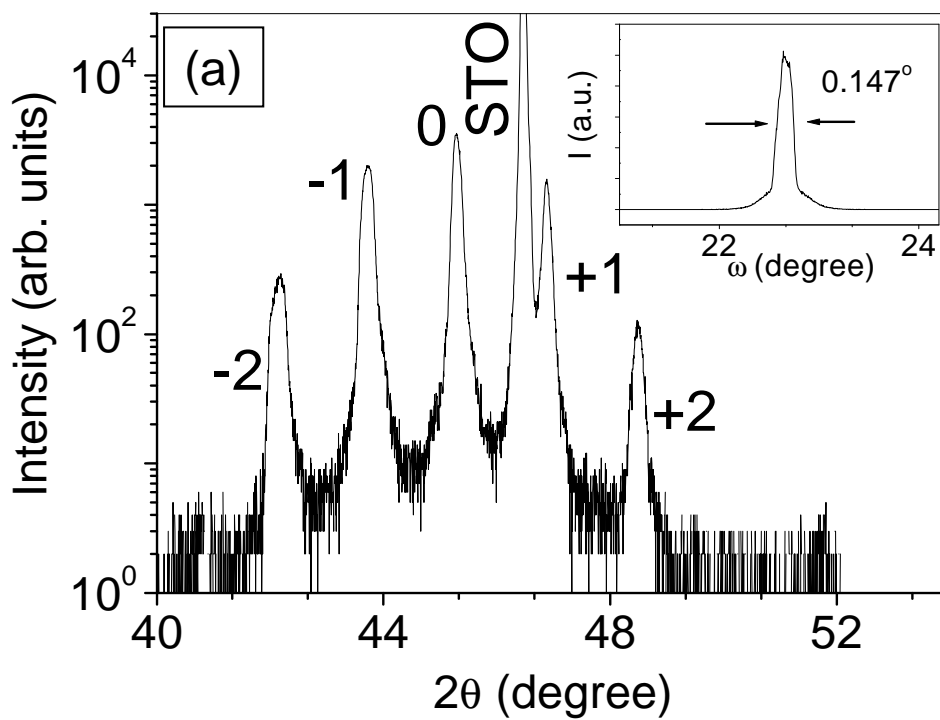
Figure captions:

Figure 1: (a) Θ - 2Θ XRD pattern of a (5/10) superlattice. Inset of Fig.1a shows the (002) rocking curve of (5/10) superlattice, (b) $M(H)$ curve of (5/10) superlattice measured at 10 K. The field is applied along the [001] direction. Inset of Fig.1b shows magnetic moment as a function of BaTiO_3 thickness at 10 K (Dots are experimental data point and solid line is just for guiding eyes). The magnetic moment of a LCMO (5 u.c.) is 3.10^{-3} emu/cm².

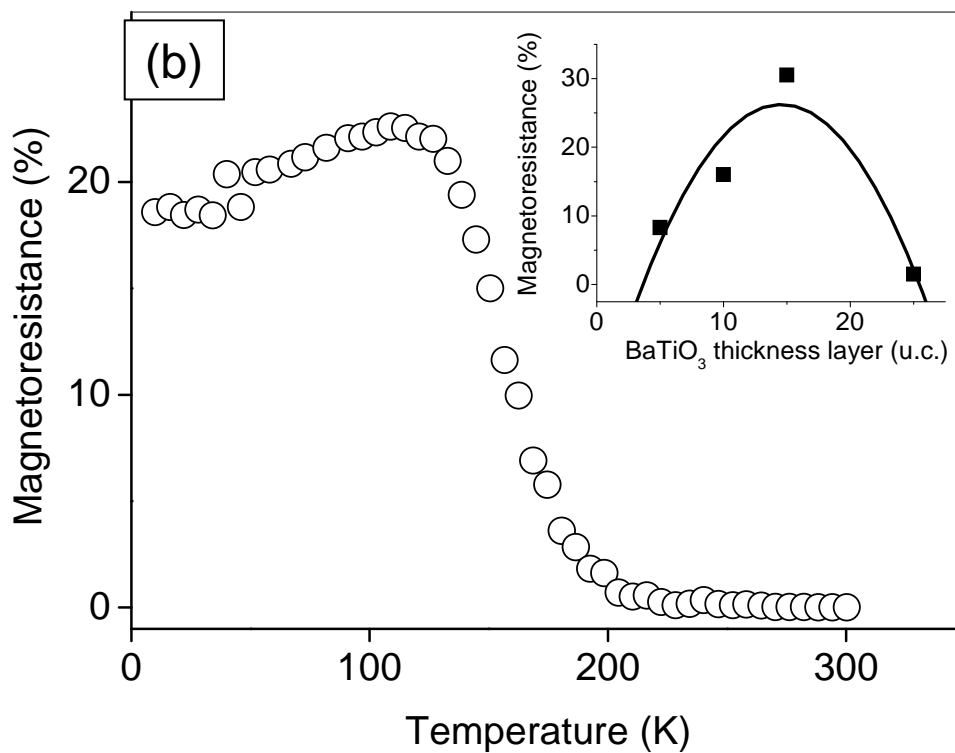
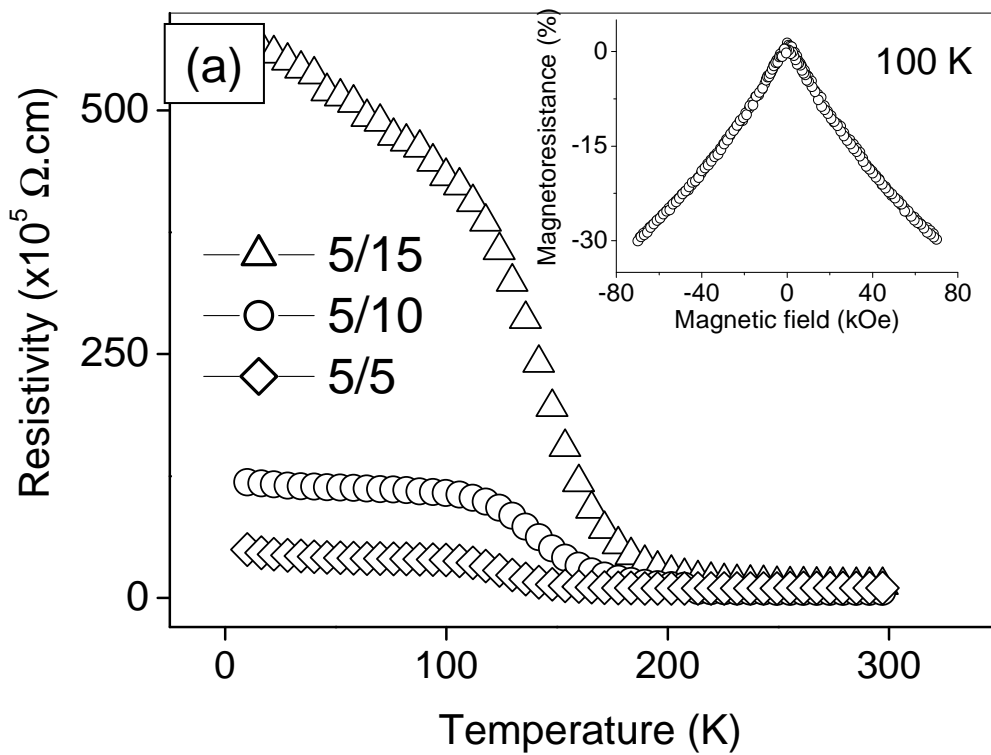
Figure 2: (a) DC $\rho(T)$ for different superlattices at zero magnetic field, (b) $MR(T)$ of (5/15) superlattice extracted from 0T and 5T ρ data. Inset of Fig.2a shows MR of (5/15) superlattice at 100K and Inset of Fig.2b is the MR measured at 100 K as a function of the BaTiO_3 spacer layer.

Figure 3: Modulus of complex impedance (Z) vs frequency with applied magnetic field at different temperatures of (5/15) superlattice. Full dots : 0T, open dots : 5T.

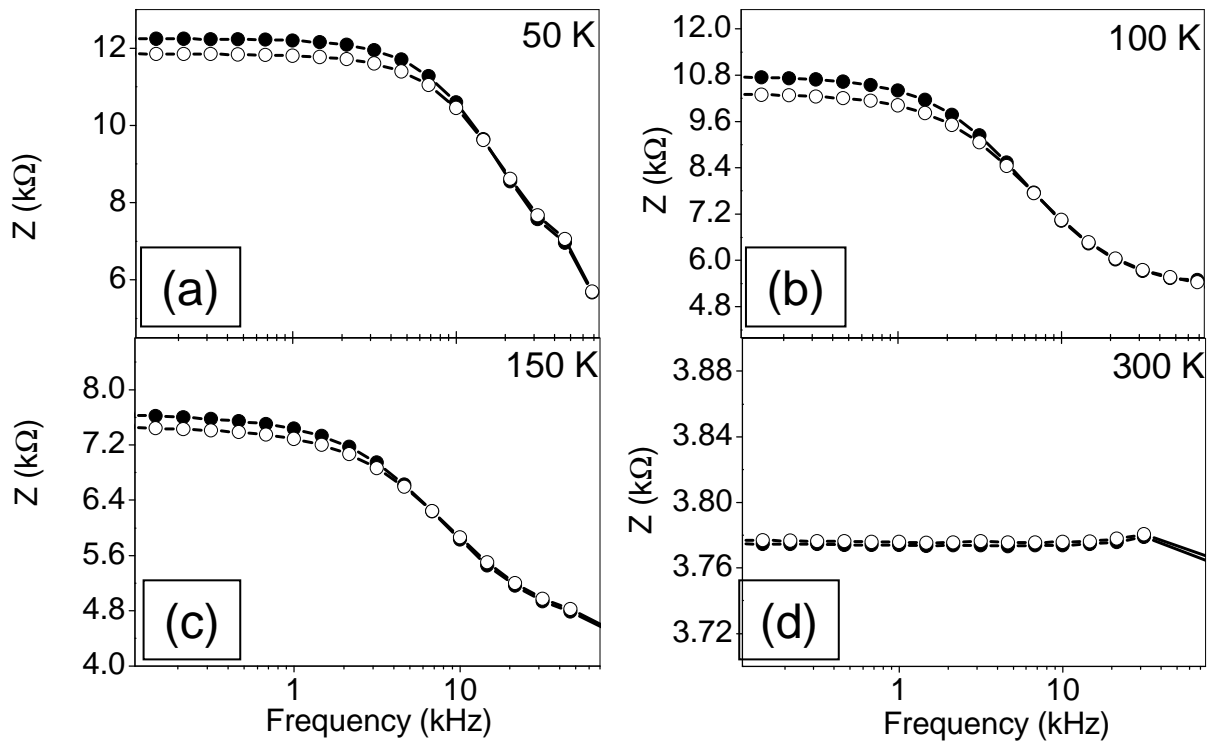
Figure 4: Capacitance vs frequency with applied magnetic field of a (5/15) superlattice at (a) 10 K, (b) 50 K, (c) 100K and (d) 150 K . Full dots : 0T, open dots : 5T.



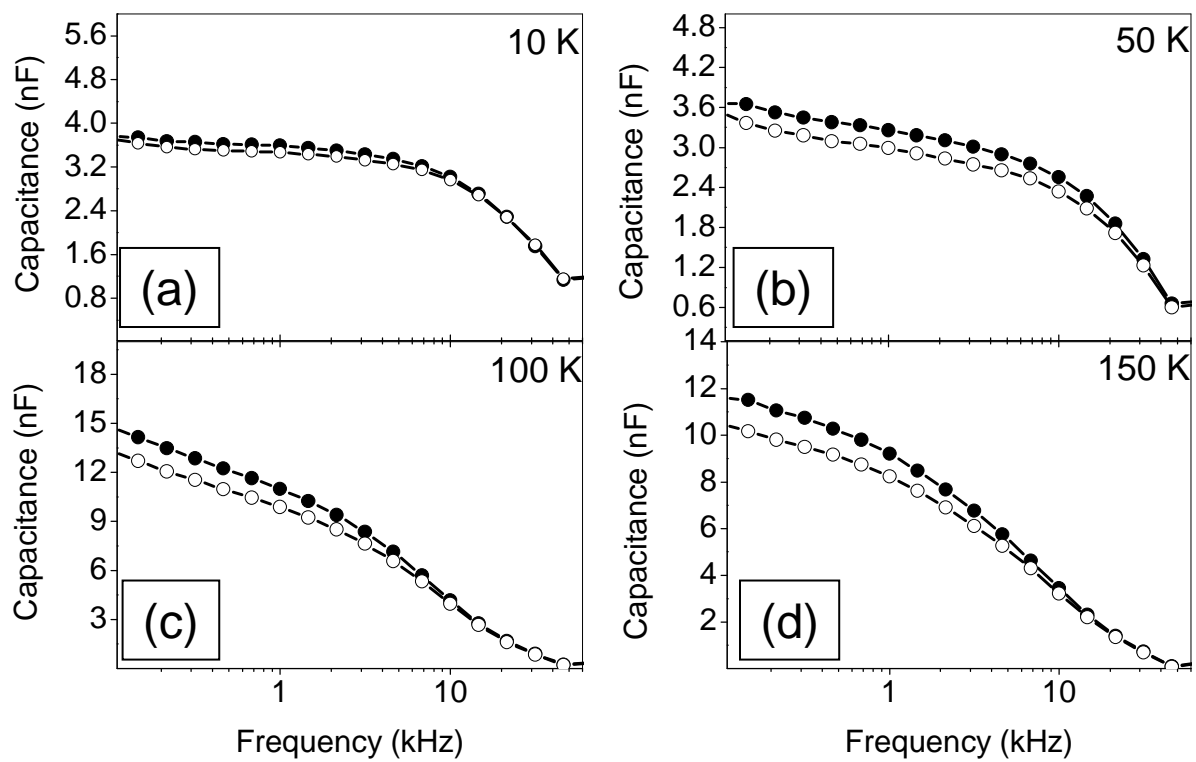
M.P. Singh et al.
Figure 1



M.P. Singh et al.
Figure 2



M.P. Singh et al.
Figure 3



M.P. Singh et al.
Figure 4